Journal of Thermal Analysis and Calorimetry, Vol. 96 (2009) 2, 419–425

INTERPRETATION OF PARTIAL THERMAL DECOMPOSITION MECHANISM OF $Dy_2(SO_4)_3 \cdot 8H_2O$
Thermal, electrical and spectroscopic techniques

S. Basavaraja[1], *A. Venkataraman*[1,*] *and Arabinda Ray*[2]

[1]Department of Materials Science, Gulbarga University, Gulbarga 585 106, India
[2]Department of Chemistry, Sardar Patel University, Vallabh Vidyanagar 388 120, India

Partial dehydration of $Dy_2(SO_4)_3 \cdot 8H_2O$ was studied employing TG, DSC, D.C. electrical conductivity and spectroscopic techniques. The possible mechanism for the loss of water molecules (partial dehydration) was found to be random nucleation obeying Mapel equation based on TG trace. The DSC traces are supports the results of TG traces and are also utilized to understand the enthalpy changes accompanying the partial dehydration and phase transition accompanying the dehydrated samples. D.C. electrical conductivity studies are attempted to supplement these TG studies. Attempts are made to explain the structural changes accompanying dehydration on the basis of infrared spectra and X-ray diffraction and scanning electron microscopic studies.

Keywords: *dysprosium sulphate hydrate, electrical behaviour, partial dehydration, structure, thermal analysis*

Introduction

Thermal dehydration and decomposition studies of metal salts [1, 2] and carboxylates [2–4] have gained significant importance. Some of the reasons for these include: the use of these compounds for the syntheses of high performance materials viz., magnetic and electrical materials employing chemie douce methods. Some of these methods include sol–gel [5, 6], decomposition of metal carboxylates [7–9], coprecipitation [10], self-propagating combustion reactions [11], etc. It was very well studied that some of the metal carboxylates and salts act as model compounds in understanding the possible mechanism for thermal dehydration and decomposition reactions [12–18].

Supplementary techniques viz., direct current electrical conductivity (D.C. electrical conductivity, σ Ohm^{-1} cm^{-1}), X-ray diffraction (XRD) and scanning electron microscopy (SEM), along with the thermal analysis viz., thermogravimetric analysis (TG), differential thermal analysis (DTA) and differential scanning calorimetry (DSC) help in understanding the structural changes taking place in the samples during the dehydration and decomposition processes [5, 6].

The oxides of rare earths such as dysprosium, samarium, lanthanum, erbium, yttrium, europium and lutetium have many important applications, such as dielectric formulation for multiplayer ceramic capacitors (MLCC) applications, high efficiency phosphor and catalysis [19–22].

Rare earth salts have gained importance for their use in the syntheses of superconducting materials, rare earth magnets and in other electronic materials. Though the thermal dehydration study was made for some of these compounds [23], a comprehensive treatment in understanding the process under different atmospheres other than static air [24, 25] was not reported and the structural changes accompanying the dehydration process were also not reported. Hence in the present investigation we report the thermal dehydration $Dy_2(SO_4)_3 \cdot 8H_2O$ in nitrogen atmosphere and the possible mechanism for this process employing supplementary techniques viz., σ, infrared spectroscopy (IR), X-ray diffraction (XRD) and SEM images to understand the solid-state changes taking place in the $Dy_2(SO_4)_3 \cdot 8H_2O$ dehydration.

Various mechanistic equations derived from Coats and Redfern (C–R) relation [26] have been employed here and are compared with the non-mechanistic equation obtained from the non-mechanistic equations [14–18]. The results of DSC traces are utilized to understand the enthalpy changes accompanying the partial dehydration and phase transition accompanying the dehydrated samples. The infrared spectra of the different hydrated forms are employed to explain the symmetry of sulphate moieties. XRD and the direct current conductivity (σ) results have been used to supplement the above studies. The σ changes taking place in the $Dy_2(SO_4)_3 \cdot 8H_2O$ during heating under different atmospheres was undertaken to know the electrical transitions. XRD pattern of the final oxide obtained from the $Dy_2(SO_4)_3 \cdot 8H_2O$ on prolonged heating was indexed.

Wendlandt [24, 25] studied the thermal dehydration behaviour under static air for $Dy_2(SO_4)_3 \cdot 8H_2O$ and

* Author for correspondence: raman_chem@rediffmail.com

1388–6150/$20.00

Akadémiai Kiadó, Budapest, Hungary
Springer, Dordrecht, The Netherlands

found that complete dehydration of this compound takes place above 350°C. However the possible mechanism (normally studied under the N_2 atmosphere) and the structural changes accompanying the dehydration process was not explained. Postmus and Ferraro [27] have reported infrared spectra of hydrated and dehydrated forms of the $Dy_2(SO_4)_3 \cdot 8H_2O$. The effect of preheating have not been clearly explained by them and supporting evidence from the other studies i.e., conductivity, XRD and SEM were not reported.

Experimental

Dysprosium sulphate of purity 99.99% was supplied by the Indian Rare Earth Ltd., Trivandrum.

The DSC traces were obtained from Dupont 950 DSC analyzer under dynamic nitrogen atmosphere with the heating rate of 10°C min^{-1} and flow rate of 100 mL min^{-1}. The TG analysis was obtained from Shimadzu DT-30 Thermal analyzer, under dynamic nitrogen atmosphere, with the heating rate of 10°C min^{-1} and flow rate of 100 mL min^{-1}. The infrared spectra of the samples in KBr pellets were recorded on a Perkin Elmer 983 spectrophotometer in the range 400–4000 cm^{-1}. The X-ray powder data were recorded on Sefert (3000) X-ray diffractometer employing CuK_α radiation.

Potential differential method employing Systronics 412 digital D.C. microvoltmeter was used for the 2-probe D.C. electrical conductivity measurement. Samples in the form of pellets of 1.0 cm diameter and 0.25 cm thickness with silver coating on both sides of the pellets were applied for electrical conductivity measurements. The mathematical calculations were performed on a computer employing a least square fit.

SEM image was taken on Lexica Steroscan Electron microscope.

Results and discussion

Thermal studies

TG trace of $Dy_2(SO_4)_3 \cdot 8H_2O$ (Fig. 1) shows the loss of five water molecules in two stages. Based on TG mass loss it was found that the first step of dehydration occurred from 110 to 150°C, corresponds to loss of three water molecules. The second step of mass loss takes place immediately thereafter and was a slow process completing at 220°C, involving loss of further two water molecule. On further heating no change in mass was observed. Though the nature of the mass loss steps observed in the present case was similar as reported by Wendlandt *et al*. [24, 25], for the thermal dehydration under static air, the loss of all eight water molecules took place in later case.

The mechanism for the partial dehydration of the five water molecules are taken together from the TG trace and was studied employing thirteen mechanistic and two non-mechanistic equations. Comparing the energy of activation E_a, frequency factor A and the correlation coefficient, r, as given in Table 1, it appears that the mechanism follows random nucleation (Mapel equation).

Different heating rates and mass changes do not appear to have substantial effect on the peak positions on the normal DSC traces, which show two distinct endotherms around 158 and 200°C (Fig. 2a). The positions of these peaks compare well with temperatures corresponding to the loss of three and two water molecules respectively observed in the TG trace (Fig. 1). However, the weak endotherm observed at around 235°C becomes more pronounced when the heating rate was 10°C min^{-1} and the mass taken was 3.2 mg. This endotherm would be probably due to a phase transition accompanying the dehydration (supported from XRD study) as TG curve does not show any further mass loss above 230°C.

The enthalpy changes (ΔH) for first and second stage of dehydration was dependent on the heating rate and mass (Table 1). At constant heating rate, the ΔH values decreases with increasing mass. The DSC trace for the first step of dehydration with the heating rate of 15°C min^{-1} show two shoulders one at 162.5 and the other at 177.5°C. The first order derivative was similar to normal DSC trace. The second order derivative (Fig. 2b) however showed two distinct peaks at 162 and 175.5°C in addition to the main endotherm indicating that the first dehydration step (removal of four water molecules) was a possible second order transition.

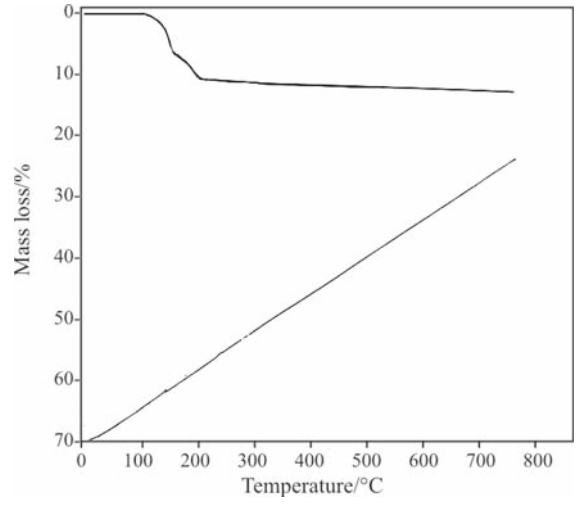

Fig. 1 TG trace for $Dy_2(SO_4)_3 \cdot 8H_2O$ sol–gel under nitrogen atmosphere

Table 1 Kinetic parameters calculated on the basis of mechanistic equations and non-mechanistic equations for thermal dehydration of $Dy_2(SO_4)_3 \cdot 8H_2O$

S1. No.	Name of the equation	Activation energy, E_a/Kcal mole^{-1}	Frequency factor, A
	1. Mechanistic equations		
1	[1] dimensional diffusion	11.956 (0.729)	$23.144 \cdot 10^4$
2	[2] dimensional diffusion	14.101 (0.730)	$26.080 \cdot 10^5$
3	Jander	17.447 (0.825)	$6.604 \cdot 10^6$
4	Brounshtein	15.157 (0.788)	$26.088 \cdot 10^5$
5	Mampel	9.988 (0.988)	$52.502 \cdot 10^3$
6	Avarmi-1	4.104 (0.802)	18.35
7	Avarmi-11	2.175 (0.726)	0.918
8	Phase boundarz reaction (cylindrical symmetry)	7.053 (0.764)	$4.117 \cdot 10^2$
9	Phage boundary reaction (spherical symmetry)	7.882 (0.764)	$4.117 \cdot 10^2$
10	Reaction order, n=1	5.137 (0.673)	43.866
11	Reaction order, n=2	2.918 (0.518)	2.215
12	Reaction order, n=3	1.707 (0.386)	0.331
13	Reaction order, n=4	9.456 (0.262)	7.676
	2. Non-mechanistic equations		
1	Coast and Redfern[11]	9.889 (0.999)	$2.28 \cdot 10^3$

The values in the parenthesis show the correlation coefficient value r

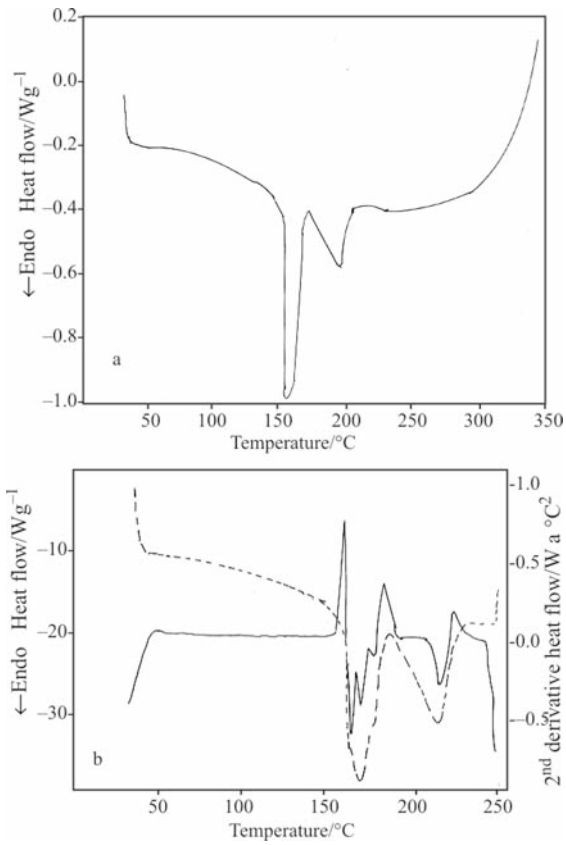

Fig. 2 a – DSC trace for $Dy_2(SO_4)_3 \cdot 8H_2O$ with sample mass 3.2 mg and ϕ=10°C m^{-1} and b – DSC trace for $Dy_2(SO_4)_3 \cdot 8H_2O$ with ϕ=15°C m^{-1} with second order derivative

Electrical conductivity

The D.C. electrical conductivity (σ, Ohm^{-1} cm^{-1}) study under different atmospheres has been found to be useful in supplementing the results of thermal studies [28, 29] in many cases. Accordingly in the present investigations the D.C. electrical conductivity of the octahydrate and the partially dehydrated samples are measured under different atmospheres with varying temperatures. Figures 3a–d show the temperature variation of electrical conductivity results for $Dy_2(SO_4)_3 \cdot 8H_2O$ under different atmospheres (static air, dynamic N_2 and dynamic N_2 containing water vapour). The conductivity (σ, Ohm^{-1} cm^{-1}) under static air atmosphere shown in Fig. 3a, remains almost constant till 118°C, it decreases till the temperature reaches 137°C. The σ value then remains constant upto 198°C. This behaviour in the region of 118 and 190°C was associated with two-step dehydration process. The thermal study shows that at this temperature five water molecules are lost. Afterwards the σ value increases slowly till the temperature was raised to around 275°C. This region corresponds to the extrinsic semiconductivity. On further rise of temperature the σ increases linearly showing intrinsic semiconductivity. The cooling curve also follows the same pattern as the heating curve of the partially dehydrated sample (containing three water molecules). Henceforth this partially dehydrated sample will be designated as AVR1.

The conductivity of the sample AVR1 was again measured under static air atmosphere after equilibrating

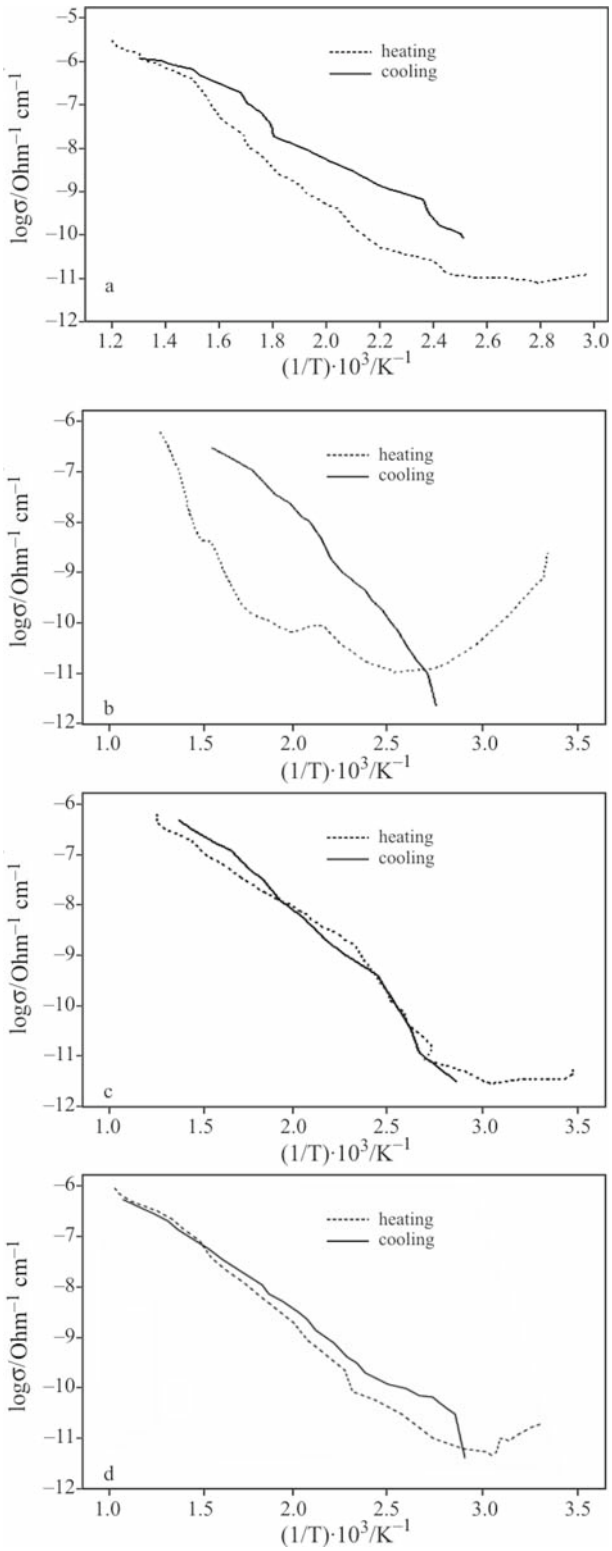

Fig. 3 D.C. electrical conductivity trace under static air atmosphere for a – $Dy_2(SO_4)_3 \cdot 8H_2O$, b – AVR1, c – AVR2 sample under dynamic N_2 atmosphere, d – AVRN sample under dynamic N_2 atmosphere containing water vapour

with water vapour for 24 h at room temperature. The value σ after initial decrease of upto 80°C (Fig. 3b), corresponding to loss of physically adsorbed water, remains constant upto 125°C. Part of water adsorbed by AVR1 has gone into coordination sphere and was lost in two-step processes in the range 125 to 280°C. Thereafter the pattern of σ increases showing intrinsic semiconductivity behaviour. The cooling curve shows a linear decrease. The sample remaining after the observation was designated as AVR2 hereafter.

Now the variation of σ with temperature for compound AVR2 under dynamic flow of N_2 was investigated (Fig. 3c). A steep decrease in σ was observed initially around 30°C corresponding to loss of small amount of water, which has been physically adsorbed. σ, then remains constant till 72°C followed by extrinsic semiconducting behaviour upto 240°C without any significant change of behavioural patterns. Above this temperature the sample shows intrinsic semiconducting behaviour. The cooling curve follows the heating curve. The sample remaining after this investigation was designated as AVRN. The sample AVRN was now subjected to conductivity measurements under dynamic N_2 containing water vapour atmosphere. The σ, decreases initially (Fig. 3d) due to the loss of adsorbed water molecules at around 60°C. The σ starts steadily increases till 200°C, followed by intrinsic behaviour.

The cooling curve is similar to the heating curve upto 140°C. There was a broadening at around 130 to 150°C in the cooling curve. This may be attributed to adsorption of water from the dynamic water vapour atmosphere.

All the experiments in electrical conductivity σ clearly indicate that water present in $Dy_2(SO_4)_3 \cdot 8H_2O$ acts as an impurity in the low temperature region (below 280°C) thereby showing extrinsic semiconducting behaviour. The possible reason for this behaviour may be that the water molecules act as electron sink, accepting electrons from $Dy_2(SO_4)_3$.

Infrared spectral studies

The infrared spectral studies of $Dy_2(SO_4)_3 \cdot 8H_2O$ and various preheated samples of it are taken in the range 400–4000 cm^{-1} (not shown in the paper). The infrared spectrum of the octahydrate shows broad and strong absorption for the O–H stretching in the region 3100 to 3600 cm^{-1}. In the trihydrate the absorption due to OH stretching was observed in the region 3100-3500 cm^{-1}. This lowering of OH stretching may be ascribed to the H_2O acting as electron sink as mentioned earlier. The migration of electron from $Dy_2(SO_4)_3$ to the antibonding orbital of H_2O will decrease OH bond order and thereby decreasing O–H

Table 2 Data from DSC traces (under N_2 atmosphere) for partial thermal dehydration and phase transformations for $Dy_2(SO_4)_3 \cdot 8H_2O$

Sl. No.	Sample mass/mg	Heating rate/°C m^{-1}	Peak 1 Peak temp./ΔH/J g^{-1}	Peak 2 Peak temp./ΔH/J g^{-1}	Peak 3 Peak temp./ΔH/J g^{-1}
1	5.0	5	155.64 (1995.0)	186.54 (724.7)	…. (---)
2	3.2	10	160.58 (2175.0)	199.23 (1065)	235.09 (133.2)
3	4.7	10	160.78 (1800.0)	202.49 (907.8)	….(---)
4	5.5	15	167.37 (1252.0)	211.82 (951.6)	…. (---)

....indicate absence of the peak and (---) the value of ΔH is not possible, as peak was not observed

stretching. In the present investigation two bands are observed at 1640 and 1610 cm^{-1} for the O–H bending mode in the octahydrate while Postmus and Ferraro [27] reported the existence of only one band at 1640 cm^{-1} for OH bending in the same. The existence of the two O–H bending may be traced to the presence of two different types of water molecules in the octahydrate.

For octahydrate a fairly large number of bands in the range 600 to 900 cm^{-1}, the absorption at 1010 cm^{-1} and the very broad absorption in the region 1080–1200 cm^{-1} osberved may all be assigned to sulphate moiety. It appears that symmetry of the sulphate in this compound was lower than T_d, the presence of C_{3v} sulphate cannot be completely eliminated. The occurrence of two bands at 1045 and 1520 cm^{-1} in the octahydrate are difficult to explain. Postmus and Ferraro [27] however have not reported these bands. May be overtones are responsible for these absorptions.

The dehydration of the octahydrate as observed in the present study was somewhat different from that reported earlier by Postmus and Ferraro [27]. As the octahydrate was heated upto 150°C (designated as AK1), three molecules of water are lost as indicated by the TG study. This sample when further heated to 220°C (designated as AK2), looses two more molecule of water and the remaining three water molecules are retained by the sample even upto 600°C. Postmus and Ferraro [27] have however reported the formation of anhydrous $Dy_2(SO_4)_3$ at 350°C for this sample.

Most of the frequencies observed for the octahydrate was present in the infrared spectra of the samples preheated under N_2 atmosphere upto 300°C (designated as AK3). In the infrared spectra of the AK1 and AK2 samples two peaks were observed in the O–H bending region, while only one peak around 1630 cm^{-1} was observed for this mode in the sample AK3. So, apparently it looks that the water molecules present in the sample AK3 are all equivalent, which otherwise would have shown a doublet at 1655 and 1650 cm^{-1} due to the presence of different types of water molecules, as observed in case of calcium malonate dihydrate [30]. The bands around 1405 and 1510 cm^{-1} however are present in all these three samples. In the infrared spectra of the samples AK1, AK2 and AK3 the width of the absorption in the region 1080–1200 cm^{-1} diminishes compared to the octahydrate. This may due to the loss of adsorbed water thereby leading to the consequent decrease in the extent of hydrogen bonding with the sulphate and change of symmetry of the sulphate moiety. The infrared spectra of the sample preheated to 400 (designated as AK4) and 600°C (designated as AK5) still show the distinct presence of water as evident from the broad absorption of the O–H stretching. Interestingly, both AK4 and AK5 samples show a band at 1630 cm^{-1} for O–H bending, probably indicating the presence of only one type of water molecules as discussed earlier. The position of the bands due to sulphate moiety in the ranges 1000–1300 cm^{-1} and 600–700 cm^{-1} in these samples AK4 and AK5 favour more of a C_{2v} (or lower) symmetry for the sulphate [31, 32].

The absence of bands at 1405 and 1520 cm^{-1} in AK4 and AK5 clearly indicate that these two samples have different symmetry from the other samples, AK1, AK3 and the parent octahydrate.

It may be mentioned here again that the DSC results do show a phase transition in the temperature region 220–265°C. The infrared spectra of the samples preheated to 300°C show the indication of phase change, but this was more pronounced in the infrared spectrum of the sample preheated above 300°C. Even at 600°C, the Dy-salt retains water molecules, but it was difficult to conclude about the nature of water molecules present. Probably the water molecules are trapped in the crystal lattice in such a way that its removal requires far more energy than the usual coordinated water. However, the sample preheated to 1000°C for 30 h did not show presence of any water molecules on the infrared spectrum. This was also evident from the monophasic Dy_2O_3 pattern observed on the XRD pattern (Fig. 4e).

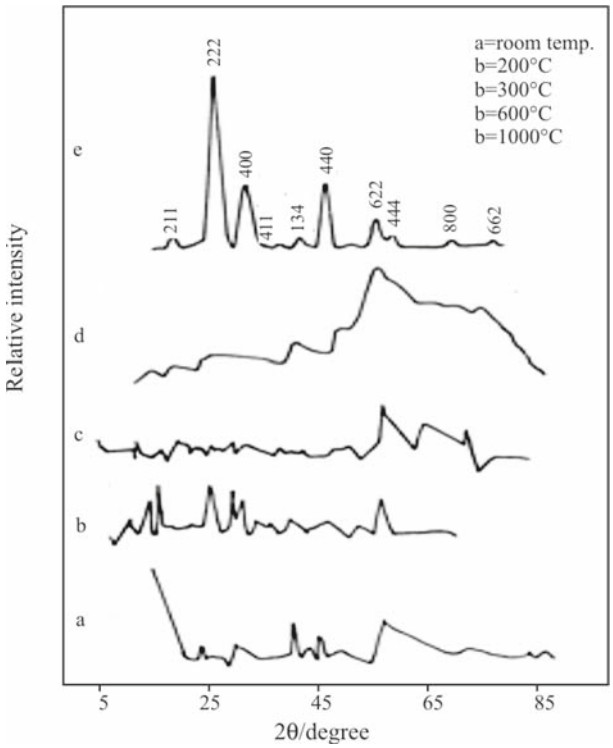

Fig. 4 X-ray diffraction patterns for $Dy_2(SO_4)_3 \cdot 8H_2O$ and its preheated samples, a – $Dy_2(SO_4)_3 \cdot 8H_2O$, b – preheated to 200°C, c – 400°C, d – 600°C and e – prolonged heating to 1000°C

X-ray diffraction studies

The X-ray diffraction patterns of the parent $Dy_2(SO_4)_3 \cdot 8H_2O$, the Dy-salt preheated to 200, 400, 600°C for 2 h and 1000°C for 30 h, respectively, are shown in Figs 4a–e. The X-ray pattern shows that the sample progressively loses crystallinity with rise of temperature. Crystallinity was completely lost for the sample preheated to 600°C. As the preheated samples showed different X-ray patterns, it may be conclusively understood that the dehydration followed here is not topotactic but involves bulk structural changes. The sample preheated to 1000°C for 30 h resembles the pattern for monophasic Dy_2O_3 having cubic symmetry (ASTM file no. 43-1006). Hence, it is understood that the Dy-salt converts to monophasic Dy oxide (Dy_2O_3) only after heating for considerable amount of time at 1000°C [33, 34].

Scanning electron micrograph (SEM)

The SEM image for the Dy_2O_3 was shown in Fig. 5. The particles are coarse with spherical shaped. The sizes of these particles are around 100 nm.

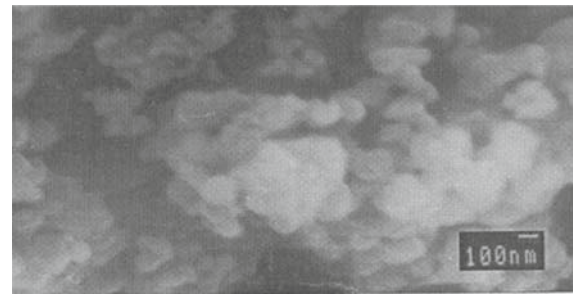

Fig. 5 SEM image of Dy_2O_3 obtained on prolonged heating of $Dy_2(SO_4)_3 \cdot 8H_2O$

Conclusions

From the present investigations following observations are made:

- The thermal dehydration under different atmospheres for $Dy_2(SO_4)_3 \cdot 8H_2O$ behaves differently. The mechanism of partial dehydration under N_2 atmosphere was understood. However as the process of the dehydration under these two atmospheres was different, it may be said with caution about the feasibility for use of $Dy_2(SO_4)_3 \cdot 8H_2O$ as model compound in the study of thermal dehydration mechanism.
- On successive dehydration by heat treatments of the $Dy_2(SO_4)_3 \cdot 8H_2O$ sample, the crystallinity was slowly lost and on final prolonged preheating the $Dy_2(SO_4)_3 \cdot 8H_2O$ was converted to monophasic Dy_2O_3 with cubic symmetry. Also, the dehydration process is not topotactic but involves bulk structural changes.
- The infrared spectra for the samples having three water molecules remaining after partial dehydration show presence of only one bending O–H mode (~1630 cm^{-1}), indicating only one type of water molecules present in the partially dehydrated sample i.e., $Dy_2O_3 \cdot 3H_2O$.
- Supplementary techniques play an important role in understanding the progress of dehydration reactions and decomposition reactions.

Acknowledgements

Authors wish to thank University Grants Commission, New Delhi (UGC Innovative Programme in Materials Chemistry) for financial assistance. One of the authors S. Basavaraja acknowledges the University Grants Commission (UGC), New Delhi for financial assistance.

References

1 I. R. Collins and S. E. Taylor, J. Mater. Chem., 2 (1992) 1277.

2 V. Logvinenko, L. Yudanova, N. Yudanova and A. Chekhova, J. Therm. Anal. Cal., 74 (2003) 395.
3 K. S. Rane, A. K. Nikumbh and A. J. Mukhedkar, J. Mater. Sci., 16 (1981) 2387.
4 D. N. Bohosale, U. Y. Patil, K. S. Rane, R. R. Mahajan, P. P. Bakare and S. R. Sawanth, Thermochim. Acta, 316 (1998) 159.
5 C. N. R. Rao, Chemical Approaches to the Synthesis of Inorganic Materials, Wiley Eastern Limited, New Delhi 1994.
6 F. R. Sale, Novel Synthesis and Processing of Ceramics, British Ceramic Society Proceedings No. 53, 1994 (U.K: The Institute of Materials).
7 M. M. Rahaman and A. Venkataraman, J. Therm. Anal. Cal., 68 (2002) 91.
8 M. E. Brown, Thermochim. Acta, 10 (1987) 153.
9 M. E. Brown and A. K. Galwey, Thermochim. Acta, 29 (1979) 129.
10 J. Gopalkrishnan, N. S. P. Bhuvanesh and A. R. Raju, Chem. Mater., 6 (1994) 373.
11 A. Venkataraman, V. A. Hiremath, S. K. Date and S. D. Kulkarni, Bull. Mater. Sci., 24 (2001) 617.
12 K. Krishnan, K. N. Ninan and P. M. Madhusudanan, Thermochim. Acta, 89 (1985) 295.
13 M. C. Patel, A. Ray and A. Venkataraman, J. Phys. Chem. Solids, 58 (1997) 749.
14 A. Venkataraman, N. V. Sastry and A. Ray, J. Phys. Chem. Solids, 53 (1992) 681.
15 A. Venkataraman and M. C. Patel, Thermochim. Acta, 242 (1994) 249.
16 M. E. Brown and A. K Galwey, Anal. Chem., 61 (1989) 1136.
17 J. Šesták, Thermochim. Acta, 203 (1992) 203.
18 A. K. Galwey, M. A. A. Mohmamad and M. E. Brown, JCS Faraday Trans, 84 (1988) 57.
19 H. Kishi, Y. Mizuno and H. Chazono, Japanese J. Appl. Phys., 42 (2003) 1.
20 R. P. Rao, J. Electrochem. Soc., 143 (1996) 189.
21 S. Eridie and R. Roy, Mater. Res. Bull., 30 (1995) 145.
22 K. S. Rane, H. Uskaikar, R. Pednekar and R. Mhalsikar, J. Therm. Anal. Cal., 90 (2007) 627.
23 J. R. Locatelli, E. C. Rodrigues, A. B. Siqueira, E. Y. Ionashiro, G. Bannach and M. Ionashiro, J. Therm. Anal. Cal., 90 (2007) 737.
24 W. W. Wendlandt, J. Inorg. Nucl. Chem., 7 (1958) 51.
25 W. W. Wendlandt and T. D. George, Inorg. Nucl. Chem., 19 (1961) 245.
26 A. W. Coats and J. P. Redfern, Nature, 201 (1964) 69.
27 C. Postmus and J. R. Ferraro, J. Chem. Phys., 48 (1968) 3605.
28 A. Venkataraman and A. J. Mukhedkar, J. Thermal Anal., 36 (1990) 1495.
29 W. W. Wendlandt, Thermochim. Acta, 1 (1970) 11.
30 E. V. Brusau, G. E. Narda and J. C. Pedregosa, J. Solid-State Chem., 143 (1999) 174.
31 J. R. Ferraro and A. Walker, J. Chem. Phys., 42 (1965) 1278.
32 J. R. Ferraro, Low Frequency Vibrations of Inorganic and Coordination Compounds, Plenum Press, New York 1971.
33 Happy, A. I. Y. Tok, F. Y. C. Boey, R. Huebner and S. H. Ng, J. Electroceram., 17 (2006) 75.
34 A. A. Dakhel, Cryst. Res. Technol., 41 (2006) 800.

Received: May 28, 2008
Accepted: June 30, 2008
Online First: February 4, 2009

DOI: 10.1007/s10973-008-9320-8